

See discussions, stats, and author profiles for this publication at: <https://www.researchgate.net/publication/263616041>

Modelling and simulation of a simple homopolar motor of Faraday's type

Article · January 2011

DOI: 10.2298/FUEE1102221B

CITATIONS

0

READS

398

4 authors, including:



[Konstantin Weise \(née Porzig\)](#)

Max Planck Institute for Human Cognitive and ...

33 PUBLICATIONS 51 CITATIONS

[SEE PROFILE](#)



[Hartmut Brauer](#)

Technische Universität Ilmenau

122 PUBLICATIONS 753 CITATIONS

[SEE PROFILE](#)

Some of the authors of this publication are also working on these related projects:



Lorentz force eddy current testing [View project](#)

All content following this page was uploaded by [Konstantin Weise \(née Porzig\)](#) on 03 July 2014.

The user has requested enhancement of the downloaded file.

Modelling and Simulation of a Simple Homopolar Motor of Faraday's Type

Dedicated to Professor Slavoljub Aleksić on the occasion of his 60th birthday

**Hartmut Brauer, Marek Ziolkowski, Konstantin Porzig,
and Hannes Toepfer**

Abstract: During the application of simulation tools of computational electromagnetics it is sometimes difficult to decide whether the problems can be solved by the computation of electromagnetic fields or circuit simulation tools have to be applied additionally. The paper describes a typical situation in an electromagnetic CAD course, not only for beginners. The modelling and numerical simulation of a simple homopolar motor, similar to that what has been presented by Michael Faraday in 1821 firstly, was used as an example. To simulate the current flow in the permanent magnet the FEM software codes COMSOL Multiphysics including the integrated SPICE module and MAXWELL have been used. The correct simulation of the entire electric circuit as well as the precise modelling of the impressed current and of the electrode contacts turned out to be very important.

Keywords: Homopolar motor; homopolar generator; Faraday's motor principle; FEM software.

1 Introduction

As is so often the case with invention, the credit for development of the electric motor is belongs to more than one individual. It was through a process of development and discovery beginning with Hans Christian Oersted's discovery of electromagnetism in 1820 and involving additional work by William Sturgeon,

Manuscript received on June 8, 2011.

The authors are with Ilmenau University of Technology, Faculty of Electrical Engineering and Information Technology, Dept. Advanced Electromagnetics, Helmholtzplatz 2, P.O.Box 100565 D - 98684 Ilmenau, Germany (e-mails: [hartmut.brauer, marek.ziolkowski, konstantin.porzig, hannes.toepfer]@tu-ilmenau.de).

Joseph Henry, Andre Marie Ampere, Michael Faraday, Thomas Davenport and a few others.

Using a broad definition of "motor" as meaning any apparatus that converts electrical energy into motion, most sources cite Faraday as developing the first electric motors, in 1821. They were useful as demonstration devices, but that is about all, and most people would not recognize them as anything resembling a modern electric motor.

Thus we nowadays usually say, that in 1821, a year after Oersted discovered electromagnetism, the great scientific thinker Michael Faraday figured out how to turn it into motion, thus creating the world's first motor [1, 2]. This discovery has changed the course of history, or at least that of electrical engineering!

Although a tremendous quantity of effort has been invested towards research on the homopolar phenomenon, still today after about 190 years following its identification by Faraday, very little information has been made public and its usage has not yet found its way into our daily lives.

The goal of this paper is to bring some insight on the working principles of Faraday's motor which by definition is employing the homopolar phenomenon. It will be demonstrated how the rather "simple design" of the Faraday motor (respectively a slightly modified homopolar motor) can be used to study the entire complexity of the modelling and numerical simulation of such simple electrical device by means of tools of computational electromagnetics (CEM). Thus, it is also a goal to describe that situation students of electrical engineering are faced to if they try to apply some commercial CEM codes to the solution of a seemingly simple technical problem.

2 Faraday's Motor

In 1821, a year after *Hans Christian Oersted* discovered electromagnetism, the great scientific thinker Michael Faraday figured out how to turn it into motion, thus creating the world's first motor. Though a primitive device that served no practical purpose, it was a great leap for humankind and led to the much more sophisticated motors of today.

The motors were constructed of a metal wire suspended in a cup of mercury (see Fig. 1). Protruding up from the bottom of the cup was a permanent magnet. In the left cup the magnet was attached to the bottom with a piece of thread and left free to move, while the metal wire was immobile. On the right side, the magnet was held immobile and the suspended wire was free to move.

When current from an electric battery applied to the wire, the circuit was completed via the mercury (a good conductor of electricity) and the resulting current

flowing through the wire produced a magnetic field. The electromagnetic field interacted with the existing magnetic field from the permanent magnet, causing rotation of the magnet on the left, or of the wire on the right (Fig. 1).

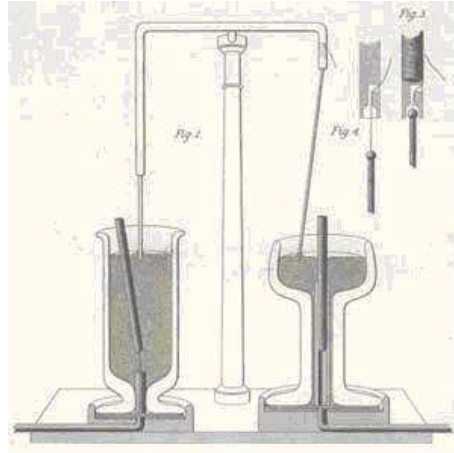


Fig. 1. The first electric motor - Michael Faraday, 1821 (from [1]).

When current ran through the circuit, it generated a circular magnetic field around the wire (the phenomenon discovered by Oersted). The wire's magnetic field interacted with a second force built into the instrument, the magnetic field of a permanent magnet fixed to the center of the dish.

Fabled experimenter Michael Faraday decided to confirm or refute a number of speculations surrounding Oersted's and Ampere's results. Faraday set to work devising an experiment to demonstrate whether or not a current-carrying wire produced a circular magnetic field around it, and in October of 1821 succeeded in demonstrating this.

When he connected a battery to form a circuit, the current-carrying wire circled around the magnet. Faraday then reversed the setup, this time with a fixed wire and a dangling magnet - again the free part circled around the fixed part. This was the first demonstration of the conversion of electrical energy into motion, and as a result, Faraday is often credited with the invention of the electric motor.

Nevertheless, we have to have in mind that Faraday's electric motor is really just a lab demonstration and it cannot be applied for useful work.

3 DC Motors

At the most basic level, electric motors exist to convert electrical energy into mechanical energy. This is done by way of two interacting magnetic fields, one sta-

tionary, and another attached to a part that can move. A number of types of electric motors exist, but most use DC motors in some form or another. DC motors have the potential for very high torque capabilities (although this is generally a function of the physical size of the motor), are easy to miniaturize, and can be "throttled" via adjusting their supply voltage. DC motors are also not only the simplest, but the oldest electric motors.

The basic principles of electromagnetic induction were discovered in the early 1800's by Oersted, Gauss, and Faraday. By 1820, Hans Christian Oersted and Andre Marie Ampere had discovered that an electric current produces a magnetic field. A number of men were involved in the work, so proper credit for the first DC motor is really a function of just how broadly you choose to define the word "motor".

3.1 Homopolar motor

The homopolar electric generation process refers to a moving electric conductor enclosed by a unidirectional and constant magnetic field. In this phenomenon, there is a compulsory relationship between the electric field, magnetic field and inertia. The generated electric power is directly determined by their magnitude. Every time when there is a flowing electric current also a magnetic field exists and vice versa.

Furthermore, inertia is the consequence of a moving mass in the surrounding space (these days also called aether). It is well recognized that the empty space is actually a fluid medium of extreme energetic density having strong inertial qualities.

Another immediate observation is made when a force is imparted to a mass: the mass accelerates and continues on its course indefinitely unless made to stop. It could be proposed that the reason for this is due to the relation of the mass constituent atoms with the medium, creating a flow of the latter, in the same direction and velocity as the displacing mass.

Since a relative movement is absolutely required in order to have an electric induction, this would suggest that it is rather the aether flow which is the subjacent working principle. The opposite is also demonstrable in the case of a motor. A flowing current with a perpendicular magnetic field will provoke a flowing medium and subsequently the object will be carried away by this flow.

The homopolar generation principle goes as follow: Electricity is generated when an electric conductor is moving while being submerged in a magnetic field. Briefly, if the movement of the electric conductor is perpendicular to the magnetic field, then the generated electrical current will start flowing in a direction perpendicular to the two first. The same is also true when applied to a motor, only the electrical polarity changes since now electricity is supplied to the motor.

Since the electrical energy produced by the homopolar generator is a pure direct current (DC) such as with a battery, the power is constant and always optimum. Furthermore, the generated tension (Volt) is not affected by the amount of current (Ampere) which is drained from the generator, contrary to any other power source, and the power generation process is not reflected back to the prime mover as an additional work load. When applied as a motor, the motive torque is constant, immediate and always optimum.

A homopolar motor has a magnetic field along the axis of rotation and an electric current that at some point is not parallel to the magnetic field. The name *homopolar* refers to the absence of polarity change. Homopolar motors necessarily have a single-turn coil, which limits them to very low voltages. This has restricted the practical application of this type of motor (Fig. 2).

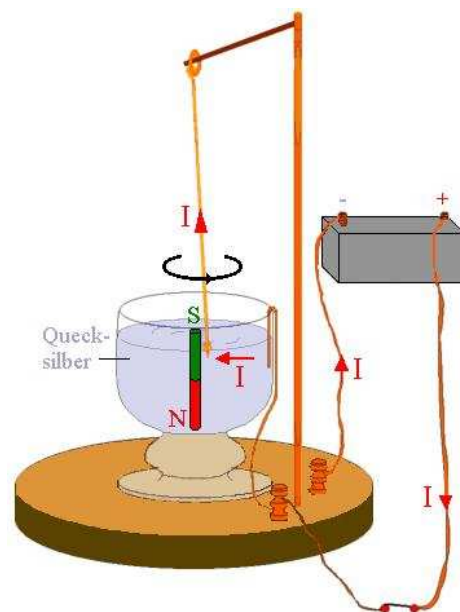


Fig. 2. Faraday's motor principle.

It is not necessary for the magnet to move, or even to be in contact with the rest of the motor; its sole purpose is to provide a magnetic field that will interact with the magnetic field induced by the current in the wire. However, the magnet must be made of a conductive material if it is being used to complete the battery-wire circuit. One can attach the magnet to the battery and allow the wire to rotate freely while closing the electric circuit even at the axis of rotation. Again, where at some point along the electric loop the current in the wire is not parallel to the magnetic field, there occurs a Lorentz force that is perpendicular to both. This Lorentz force

is tangential and produces a torque in the wire, so that the wire rotates. In contrast to other electrical motors, both the orientation and magnitude of the magnetic field and the electric current do not change.

Like most electro-mechanical machines a homopolar motor is reversible so that when electrical energy of a suitable kind is put into its terminals, mechanical energy can be obtained from its motion and vice versa. The operation of a homopolar motor is a simple consequence of the Lorentz force. In a homopolar motor the moving current carriers feel an induced force and move whereas in the side of the rotor feeling this force a torque is induced.

3.2 Homopolar generator

A homopolar generator is a DC electrical generator comprising an electrically conductive disk rotating in a plane perpendicular to a uniform static magnetic field (Fig. 3). A potential difference is created between the center of the disk and the rim, the electrical polarity depending on the direction of rotation and the orientation of the field. It is also known as a *unipolar generator*, *acyclic generator*, *disk dynamo*, or *Faraday disk*. The voltage is typically low, on the order of a few volts in the case of small demonstration models, but large research generators can produce hundreds of volts, and some systems have multiple generators in series to produce an even larger voltage. They are unusual in that they can source tremendous electric current, some more than a million amperes, because the homopolar generator can be made to have very low internal resistance.

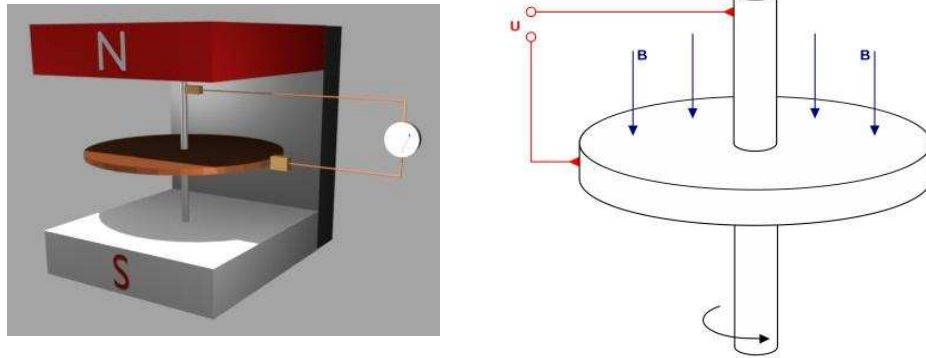


Fig. 3. Basic Faraday disk generator.

The homopolar generator was developed first by Michael Faraday during his experiments in 1831 [3]. It is frequently called *the Faraday disk* in his honor. It was the beginning of modern dynamos, i.e. electrical generators which operate using a magnetic field. It was very inefficient and was not used as a practical power

source, but it showed the possibility of generating electric power using magnetism, and led the way for commutated direct current dynamos and then alternating current alternators.

We can create a homopolar generator by replacing the cell that drove the homopolar motor with a voltmeter. Whereas the homopolar motor converts electrical energy (supplied by the cell) into mechanical energy, the homopolar generator does the reverse: providing mechanical energy to turn the disk and obtain an electromagnetic force (emf) and (if a current path exists) an electric current.

Looking to a mobile charge q travelling with the disk (with velocity \mathbf{v} at the point and time), the charge is subject to the Lorentz force $q\mathbf{v} \times \mathbf{B}$, which is towards the axle. This gives rise to an emf as indicated by the voltmeter (and a current if the circuit is closed).

Again, a homopolar generator is conceptually a little simpler than its multipole cousins but, because there is only one current path, the emf is small. (On the other hand, ideal brushes would in principle allow a large current.)

3.3 What is a homopolar motor / generator used for?

Although a tremendous quantity of effort has been invested toward research on the homopolar phenomenon, still today after about 190 years following its identification by Faraday, very little information has been made public and its usage has not yet found its way into our daily lives.

It is awkward since it is known in the scientific community that the homopolar electric generation is naturally extra-efficient. The single engineering challenge has been all along the conception of a working unit which does not cripple the generation process while tapping this freely given energy.

Homopolar motors are also called unipolar motors. These non-commutating electric motors use, in general, both alternating and direct current, and process energy that travels in one direction at all times.

The most common use of homopolar motors is in generators that are installed in electroplating process plants. The generators use direct current (DC) and low voltage, but the current in the motors is high enough to operate the heavy machinery.

Homopolar motors have been used in high-torque wind turbines. The mechanics of the motors provide a low-cost means of converting wind into electricity because of the reduced need for multidirectional gears. These motors also require less maintenance than bipolar motors.

Small engines, such as those in toy cars, can be built using homopolar motors. The spinning wheels create force, which causes the magnet to spin and create a magnetic field. This electricity flowing in one direction is used to power the engine.

There are many other instances where the homopolar phenomenon is applied if one stops and thinks about it. Our mother Earth for instance is a prime example (in perpetual motion!) and elsewhere also, such as in the case of MHD (Magnetohydrodynamics) processes and Hertzian waves [4].

4 Numerical Description of Homopolar Motor Behaviour

Homopolar motors and generators are simpler than their multipolar cousins, but are very rarely used in practice. However, they illustrate the principles nicely, and a homopolar motor is both easy to make and easy to understand. Thus, this is a nice issue to be investigated in an electromagnetic CAD course. We will use the simple homopolar motor (Fig. 5) to apply the CEM tools (FEM software, circuit analysis software) which will give us the fields, forces and torques. Because of the simplicity of the device it is possible to evaluate the features of FEM codes under test.

The permanent magnet produces a magnetic field \vec{B} that is vertically upwards through the conducting disk. The cell provides current that flows through one brush to the central shaft, then outwards to the right towards the brush on the rim. The (conventional) current density \vec{J} is subjected to a force in the direction $\vec{J} \times \vec{B}$, which is forwards, towards us. This force is transmitted to the disk, which rotates in the sense shown at right (Fig. 4).

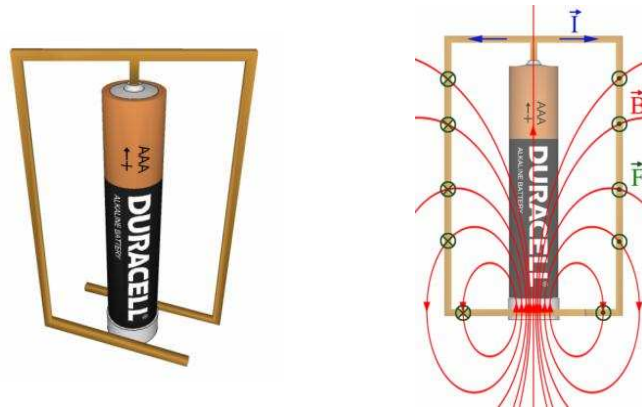


Fig. 4. Homopolar motor scheme with battery, magnetic disk and wire frame (left); flux density and forces (right).

Because there is always a current path between the brushes (or at least there would be if they were ideal), the resultant torque is steady. Note that there is only one current-carrying path, compared with many in a typical multipolar motor. On the other hand, the current could be large if the brushes had low resistance.

In a simple design for a very simple homopolar motor, the magnet itself (or its coating) touches the cell via a metallic screw and is used as the contact for the brushes. In this design, the rotor is the disk. The piece of wire includes both brushes. It uses a 1.5V cell, one of its terminals is the contact for one brush, and a cylindrical permanent magnet, its circumference is the contact for the other.

4.1 Physical modelling of the motor

Like all dynamos, the Faraday disk converts kinetic energy to electrical energy. This machine can be analyzed using Faraday's own law of electromagnetic induction. This law (in its modern form) states that an electric current is induced in a closed electrical circuit when the magnetic flux enclosed by the circuit changes (in either magnitude or direction). For the Faraday disk it is necessary, however, to consider that the circuit(s) consist of each radial "spoke" of the disk connected to the rim and center and then through the external circuit.

The Lorentz force law is more easily used to explain the machine's behaviour. This law, discovered thirty years after Faraday's death, states that the force on an electron is proportional to the cross product of its velocity and the magnetic flux vector. In geometrical terms, this means that the force is at right-angles to both the velocity (azimuthal) and the magnetic flux (axial), which is therefore in a radial direction. The radial movement of the electrons in the disk produces a charge separation between the center of the disk and its rim, and if the circuit is completed an electric current will be produced.

For our purposes, the principle of the Faraday motor has been slightly modified. On a cylindrical permanent magnet (NdFeB) with axial magnetization a metallic screw is fixed. If this is combined with a battery, the magnet will start to rotate as soon as we connect the battery and the magnet by means of a copper wire (Fig. 5). Depending on the position of the contact point of the wire on the magnet surface different rotational speeds of the magnet can be observed.

It is not necessary for the magnet to move, or even to be in contact with the rest of the motor; its sole purpose is to provide a magnetic field that will interact with the magnetic field induced by the current in the wire. However, the magnet must be made of a conductive material if it is being used to complete the battery-wire circuit. One can attach the magnet to the battery and allow the wire to rotate freely while closing the electric circuit *even at the axis of rotation*. Again, where at some point along the electric loop the current in the wire is not parallel to the magnetic field, there occurs a *Lorentz force* that is perpendicular to both. This Lorentz force is tangential and produces a torque in the wire, so that the wire rotates. In contrast to other electrical motors, both the orientation and magnitude of the magnetic field and the electric current do not change.

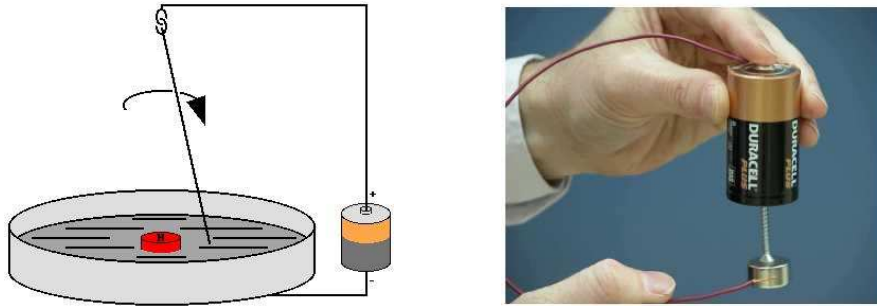


Fig. 5. A simple homopolar motor: Faraday's historical scheme (left); here used model, made with drywall screw, alkaline battery cell, wire, and neodymium magnet (right). The screw and magnet contact the bottom of the battery cell and are held up by magnetic attraction. The screw and magnet spin.

People are sometimes confused by the fact that there are no changes in the magnetic field or electric current, and no recognizable North-South pole interaction between the magnet and the electric circuit. They often think that field lines cannot be used to understand homopolar machines, or that the field lines rotate (*Faraday Paradox*). As the homopolar motor must have a current-carrying wire, any components used to complete the circuit (such as the drywall screw and the magnet in the picture above) must be made of a conducting material.

The homopolar motor can be well explained by the Faraday model of lines of force, with a tangential force (hence, a torque) resulting where the electric current makes an angle with the magnetic lines of force. Thus, the homopolar motor provides a simple demonstration of the *Lorentz force*.

4.2 Numerical modelling of the rotating magnet

First an analytical approach is used to model the rotating magnet. The geometry shown in Fig. 6 was applied for defining the parameters. The cylinder represents the Neodymium magnet ($\text{Nd}_2\text{Fe}_{14}\text{B}$), the properties are summarized in Table 1. It is assumed that the current flows directly from the screw on the top to the contact of the wire at the surface of the magnet. Both source and sink are defined to be point-like.

Table 1. Material properties and geometric parameters of the magnet.

Remanence \vec{B}	Conductivity σ	Mass Density ρ	Height h	Radius r_0
$1.3T\vec{e}_z$	$\frac{1}{140} 10^8 \frac{\text{S}}{\text{m}}$	$7\,400 \frac{\text{kg}}{\text{m}^3}$	24 mm	7 mm

The analytical description of the rotating cylindrical magnet requires the cal-

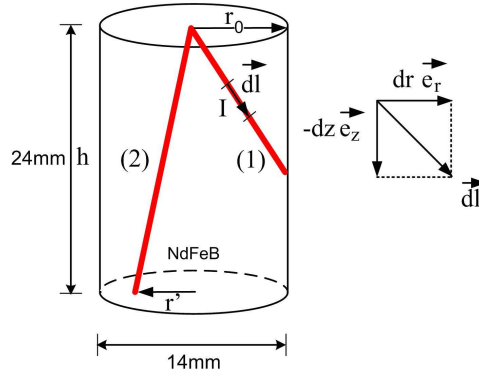


Fig. 6. Geometry of the rotating magnet used in the analytical approach. Case (1): The wire is placed on the outer shell of the magnet ($r = r_0$); Case (2): The wire is placed at the bottom of the magnet ($r = r'$).

calculation of the angular acceleration $\vec{\alpha}$. Therefore, the Lorentz force, \vec{F} , the torque \vec{M} and the moment of inertia Θ have to be determined. The Lorentz force can be calculated as follows (see Fig. 6):

$$d\vec{F} = I_0 (d\vec{l} \times \vec{b}) \quad (1)$$

$$d\vec{l} = -dz \cdot \vec{e}_z + dr \cdot \vec{e}_r \quad (2)$$

$$\vec{B} = B_0 \vec{e}_z \quad (3)$$

$$d\vec{F} = -I_0 B_0 dr \cdot \vec{e}_r \quad (4)$$

Here is I_0 the current through the wire. The torque \vec{M} is caused by the Lorentz force and can be calculated with

$$d\vec{M} = \vec{r} \times d\vec{F} \quad (5)$$

$$\vec{M} = -I_0 B_0 \int_0^r dr \vec{e}_z \quad (6)$$

The moment of inertia of the cylindrical magnet is given by

$$\Theta = \frac{1}{2} m r_0^2 \quad (7)$$

Case 1: When the conductor is placed on the surface of the cylinder (see Fig. 6) the integration of eq. (6) has to be extended to r_0 .

$$\vec{M}_1 = -\frac{1}{2} I_0 B_0 r_0^2 \vec{e}_z \quad (8)$$

To calculate the angular acceleration $\vec{\alpha}_1$ of the magnet the torque \vec{M}_1 from eq. (8) and the moment of inertia from eq. (7) have to be related by

$$\vec{\alpha}_1 = \frac{\vec{M}_1}{\Theta} \quad (9)$$

$$\vec{\alpha}_1 = \frac{I_0 B_0}{m} \vec{e}_z \quad (10)$$

Thus, in *case 1* the angular acceleration is independent of the z -position where the wire contacts the magnet.

Case 2: When the wire is placed at the bottom of the cylinder (see Fig. 6) the integration of eq. (6) has to be extended merely to $r' < r_0$.

$$\vec{M}_2 = -\frac{1}{2} I_0 B_0 r'^2 \vec{e}_z \quad (11)$$

Again the angular acceleration yields from combining the torque \vec{M}_2 from eq. (11) and the moment of inertia from eq. (7) to

$$\vec{\alpha}_2 = \frac{\vec{M}_2}{\Theta} \quad (12)$$

$$\vec{\alpha}_2 = -\frac{I_0 B_0}{m} \frac{r'^2}{r_0^2} \vec{e}_z \quad (13)$$

In the *case 2* the angular acceleration depends on the position r' of the wire.

The numerical computation of the forces and moments cannot be based on point-like contacts of the circuit on the magnet surface. Therefore, three different approaches have been applied: *the point model*, *the electrode model* and *the screw model* (see Fig. 7).

In *the point model* (a) the source and sink were defined as infinitesimal small dots, similar to the analytical approach.

In contrast, *the electrode model* (b) enlarges both to a finite size. In this case, the source was modelled as an additional cylinder (diameter of 2 mm), representing the head of the screw. Furthermore the conductor on the outer surface of the magnet was modelled as a small cylinder with diameter of 1 mm.

Finally, *the screw model* (c) is an extension of the electrode model, where geometry and material properties of the screw have been taken into account. In the computation an iron screw was assumed, with a conductivity of 1.1E+7 S/m.

During the simulations turned out that the method of defining the source parameters is very important. There can be impressed either a constant voltage

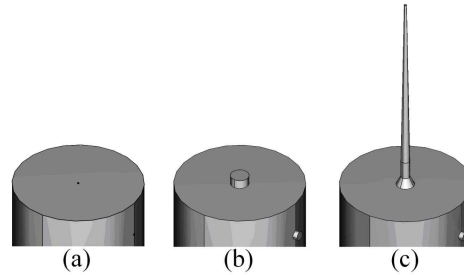


Fig. 7. Three models for describing the electric contacts to the magnet used in the numerical simulation: (a) point model, (b) electrode model, (c) screw model.

($U_0 = 1.5$ V, AA-cell) or a current. The current can be easily approximated by neglecting the resistances of the permanent magnet and of the wire. The internal resistance of the battery was estimated to $R1 = 0.15 \Omega$. This leads to an impressed current of about $I = 10$ A. The numerical simulations for the point model (a) and the electrode model (b) were performed by applying both approaches.

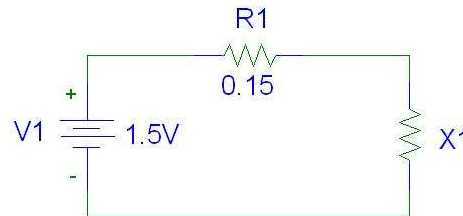


Fig. 8. Electric circuit of the rotating magnet configuration consisting of the battery with the internal resistance $R1$ and the FEM model $X1$.

In addition to fixing the voltage or the current, a third method of defining the source parameters can be used. This is the link of the FEM model to a network simulator like SPICE. Therefore, the FEM model ($X1$) is defined as a part of an electric circuit using the SPICE module of *COMSOL Multiphysics 3.5a*, where $R1$ describes the internal resistance of the battery and $V1$ the voltage source (Fig.8). Thus, the source parameters can be determined precisely by using an iterative solver. This procedure has been finally used for the screw model.

5 Numerical Simulation

Having a look on the magnetic field lines of this configuration it becomes apparent how the forces (caused by the permanent magnet and by the current flow in the wire) interacting to create the motion.

The numerical simulations have been performed with commercial finite el-

ement method (FEM) software codes, *COMSOL*TM *Multiphysics* (v3.5a) and *MAXWELL*TM (R12). By using the two different software packages there is a chance to verify the reliability of the results. The point model and the electrode model have been realized with both tools. The screw model was computed only with *COMSOL Multiphysics 3.5a* using the integrated SPICE module.

5.1 Experimental setup

The experimental setup consists of an electric battery (1.5 V, AA-cell), a cylindrical permanent magnet ($\text{Nd}_2\text{Fe}_{14}\text{B}$; $B_r = 1.3$ T), a metallic screw and a copper wire to connect the battery with the magnet (Fig. 9). The forces and the rotational speed can be determined either by means of the analytical approach or with FEM simulations. Such simulations have been made using impressed current and impressed voltage, respectively, whereas point-like contacts and extended electrodes have been modeled (Fig. 7). To analyze the different resistances of the circuit the FEM simulations using *COMSOL Multiphysics* have been combined with the integrated circuit analysis tool SPICE (Fig. 8).

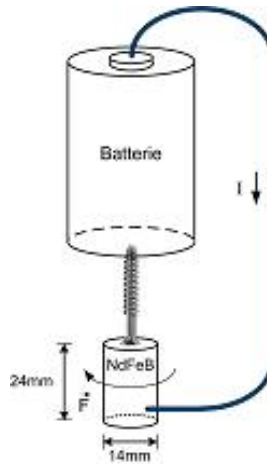


Fig. 9. Setup of the homopolar motor (Faraday motor).

5.2 Boundary conditions

The boundary conditions of the rotating magnet are all of the type "electrical insulation" $\vec{n} \cdot \vec{J} = 0$ where \vec{n} is the unit vector at the surface of the cylinder. This boundary condition holds for the whole geometry, except of the positions of the screw and the wire, i.e. the positions where the current flows into the magnet or out of it. At these boundaries the parameters of the source and sink were defined.

In the case of the point model the boundary condition of the source was defined by setting the voltage of the point lying on the top of the cylinder to $U_0 = 1.5$ V. According to this, the second point on the outer shell of the cylinder was declared to $U_{ground} = 0$ V. On the other hand, a second simulation was performed by impressing a constant current of $I_0 = 10$ A into the magnet.

In the case of the electrode model the boundary conditions were applied to the faces of the small cylinders representing the wire and the screw.

The boundary conditions for the screw model are different from the other models. The tip of the screw and the wire were defined to be of type "circuit terminal" enabling the implementation of the FEM model into an electric circuit simulated by the SPICE module of *COMSOL*.

5.3 Mesh generation

Further differences between both software packages have been arisen during realizing the point model. In *COMSOL* it is possible to create point sources, which are not available in *MAXWELL*. Therefore, the points were modelled as small cylinders with radius of 0.01mm. Furthermore, the mesh generation techniques are different in both codes. In *COMSOL* it is possible to create the mesh with desired properties, e.g. size of the elements before starting the simulations. The solver is using this predefined mesh to compute the solutions. However, in *MAXWELL* the mesh will be refined till a certain error limit is reached, i.e. the refinement per step was set to 30%, the maximum number of iterations was limited to 10, and this should lead to a maximum error limit (for the energy in the considered elements) of 1%. Because point-like contacts cannot be defined in *MAXWELL*, a small circle around the contact on the top of the cylinder and a very small cylinder on the side surface of the magnet have been designed. These artificial electrodes have been included in the mesh refinement procedure leading finally to much better results for the point model (see Fig. 7). Because of these reasons, the point model had to be realized in both software packages in different ways. This has to be taken into account when comparing the results. Only the electrode model was identically realized in both codes.

Because of the different source and sink modelling, the meshes have to be adapted for each model. Furthermore, all calculations were performed by using at least two different meshes for each model to identify any instability. The mean sizes of the finite elements for the three models are listed in Table 2. However, it is important to emphasize that the maximum element size for *MAXWELL* only affects the initial mesh.

In order to calculate the angular acceleration depending on the wire position, several FEM solutions with well-defined positions of the wire have been performed.

After each simulation, the density of the Lorentz force was calculated as follows:

$$\vec{f} = \vec{J} \times \vec{B} \quad (14)$$

and the torque \vec{M} was calculated by

$$\vec{M} = \int_V \vec{r} \times \vec{f} dV \quad (15)$$

If both quantities are known, the angular acceleration can be determined from eq. (9). All calculations have been performed using the post-processing routines of the simulation software packages.

Table 2. Maximum size of FE in different meshes created in COMSOL Multiphysics 3.5a and MAXWELL 12, used for simulations of point, electrode and screw model, respectively.

	COMSOL Multiphysics		MAXWELL	
	Cylinder	Contact/Screw	Cylinder	Contact/Screw
Point Model				
mesh #1 (coarse)	2 mm	0.05 mm	4 mm	0.005 mm
mesh #2 (fine)	2 mm	0.01 mm	1 mm	0.0025 mm
Electrode Model				
mesh #1 (coarse)	1 mm	0.3 mm	4 mm	0.2 mm
mesh #2 (fine)	0.5 mm	0.15 mm	1 mm	0.1 mm
Screw Model				
mesh #1 (coarse)	1 mm	0.3 mm	–	–
mesh #2 (fine)	0.5 mm	0.15 mm	–	–

6 Simulation Results

6.1 The screw model

In the following diagrams, the results of the screw model are presented. It was assumed that the screw model yields to the most accurate results compared to the point and the electrode model. By implementing the FEM model into an electric circuit (Fig. 8), *COMSOL* calculated an impressed current of $I_{FEM} = 9.43$ A flowing through the magnet. The voltage drop over the screw and the magnet was about $U_{FEM} = 85$ mV due to the high conductivity of the rotating magnet. This is contrary to the assumption of a source voltage of $U_0 = 1.5$ V.

Fig. 10 shows the expected quadratic dependency of the angular acceleration on the wires radial position. In Fig. 12 is shown that the angular acceleration, as

expected, does not depend on the axial position of the wire, resulting to a value of 70.4 s^{-2} . It was observed, that the simulations with two meshes yield always similar results. Therefore, the solutions for only one mesh are presented.

6.2 The point model

The results of the angular acceleration for the point model are depicted in Fig. 10 - 13. In Fig. 10 and 11 the angular acceleration depending on the wires radial position at the bottom of the magnet is shown, either for a voltage or a current source. For a voltage source, it can be seen that the solution of *COMSOL* is mesh dependent. Reason for this is the inhomogeneity of the voltage point source defined in *COMSOL*. It can be observed that a coarser mesh results in higher angular accelerations. Due to the high conductivity of the magnet, it was ascertained that the voltage drops from 1.5 V to about 0.7 V near the point source. According to this, the voltage drops from 0.7 V to 0 V at the sink. This results in large gradients of the voltage near the points. In consequence, the current density is increasing rapidly. The size of the finite elements now influences this gradient and therefore the angular acceleration. In contrast the deviations between the solutions of the two meshes for *MAXWELL* are negligible. Reason for this is the modelling of the points as small electrodes. The iterative mesh generation process of *MAXWELL* leads to nearly the same mesh to reach the error limit of 1%. Furthermore *MAXWELL* discretized the small cylinders representing the source and the sink and prevented any inhomogeneity.

In the charts of Fig. 11 and Fig. 13 these observations could not be studied for an impressed current. The mesh dependence of *COMSOL* was not observed in this case. A possible reason for this is the restriction of the current to $I_0 = 10 \text{ A}$. Furthermore both software packages calculated a similar angular acceleration along the wires position. In Fig. 13 it can be seen, that an impressed current of $I_0 = 10 \text{ A}$ leads to an angular acceleration of 75.7 s^{-2} for *COMSOL* and 75.9 s^{-2} for *MAXWELL*. Compared to the screw model this corresponds to a deviation of about 7%.

6.3 Electrode model

The results of the angular acceleration for the electrode model are depicted in Fig. 14 - Fig. 17. Because of the finite size of the source, the mesh dependence of *COMSOL* was not observed in this case. Hence, the solutions will only be presented for one mesh. The simulation results for a voltage source were leading to unusual high values. Reason for this is the assumption, that the voltage of the whole face of the source cylinder on the top of the magnet is $U_0 = 1.5 \text{ V}$. In combination

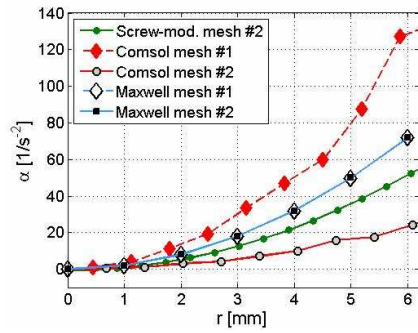


Fig. 10. Angular acceleration α of the point and screw model depending on the wires radial position at cylinder bottom (voltage source: $U_0 = 1.5$ V).

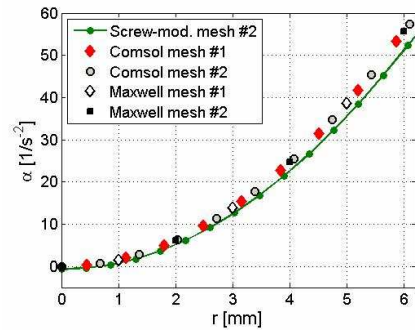


Fig. 11. Angular acceleration α of the point and screw model depending on the wires radial position at cylinder bottom (current source: $I_0 = 10$ A).

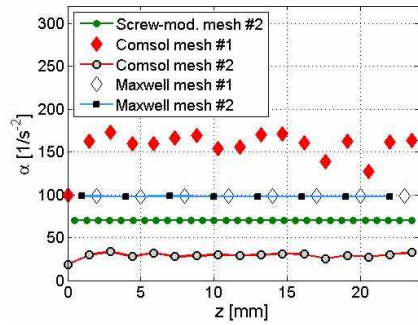


Fig. 12. Angular acceleration α of the point and screw model depending on the wires axial position along the z -axis at the cylinder surface ($z = 0$ mm corresponds to the bottom, $z = 24$ mm to the top of the cylinder; voltage source: $U_0 = 1.5$ V).

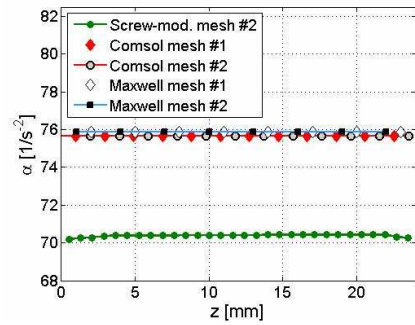


Fig. 13. Angular acceleration α of the point and screw model depend on the wires axial position along the z -axis at the cylinder surface ($z = 0$ mm corresponds to the bottom, $z = 24$ mm to the top of the cylinder; current source: $I_0 = 10$ A).

with the high conductivity of the magnet, this leads to extremely high current densities and therefore to the presented angular accelerations.

In the charts of Fig. 15 and Fig. 17 can be seen, that an impressed current yields to similar results for the electrode model compared to the point and screw model.

In Fig. 16 an increase of the angular acceleration depending on the z -position of the wire can be observed. This is due to the decrease of the resistance for wire positions near to the top of the magnet because of shorter current paths. The same effect can be observed in the other models with a current source as well. But due to scaling and significantly lower current densities this effect is less obvious.

The z -dependency of the angular acceleration for an impressed current is shown in Fig. 17. Both software packages give a similar angular acceleration along the wire positions. It was found that an impressed current of $I_0 = 10$ A leads to an angular acceleration of 75.61 s^{-2} for *COMSOL* and 74.65 s^{-2} for *MAXWELL*.

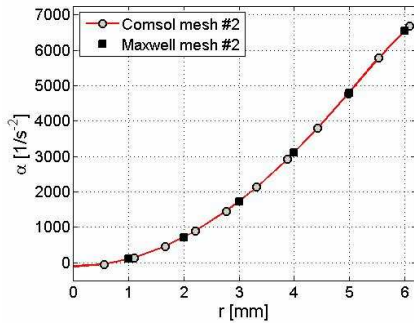


Fig. 14. Angular acceleration α of the electrode model depending on the wires radial position at cylinder bottom (voltage source: $U_0 = 1.5$ V).

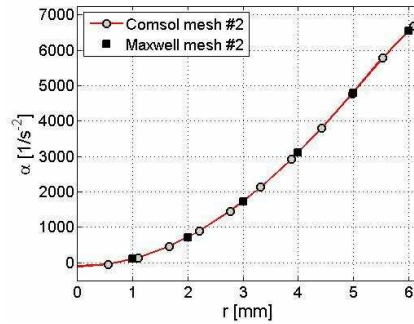


Fig. 15. Angular acceleration α of the electrode model depending on the wires radial position at cylinder bottom (current source: $I_0 = 10$ A).

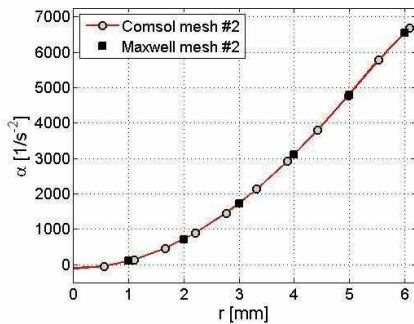


Fig. 16. Angular acceleration α of the electrode model depending on the wires axial position along the z -axis at the cylinder surface ($z = 0$ mm corresponds to the bottom, $z = 24$ mm to the top of the cylinder; voltage source: $U_0 = 1.5$ V).

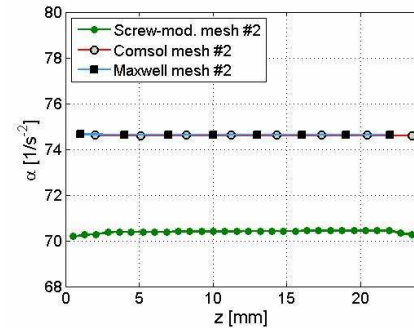


Fig. 17. Angular acceleration α of the electrode model depending on the wires axial position along the z -axis at the cylinder surface ($z = 0$ mm corresponds to the bottom, $z = 24$ mm to the top of the cylinder; current source: $I_0 = 10$ A).

7 Discussion

The simulation results of the homopolar motor revealed the importance of the combination of geometric and source modelling. The assumption of a voltage source turned out to be wrong in this case. The total voltage has to drop over the rotating

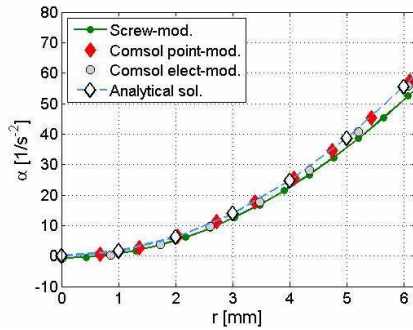


Fig. 18. Angular acceleration α of the point-, electrode- and the screw model as well as the analytical solution depending on the wires radial position (current source: $I_0 = 10\text{A}$).

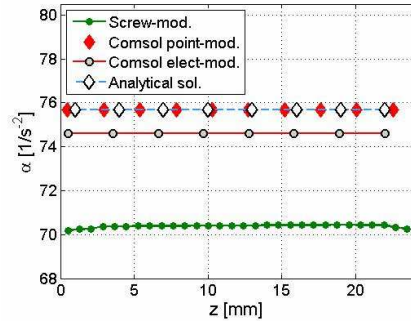


Fig. 19. Angular acceleration α of the point-, electrode- and screw model depending on the wires axial position along the z -axis on the surface of the cylinder ($z = 0\text{ mm}$ corresponds to the bottom, $z = 24\text{ mm}$ to the top of the cylinder; current source: $I_0 = 10\text{ A}$).

magnet, which is not correct due to the low resistance of the magnet. The main part of the voltage drops over the internal resistance of the battery. Thus, the results obtained with a voltage source cannot be accepted because of the high values of the angular acceleration. Furthermore, this yields in combination with a point source to unstable results with *COMSOL*, where one is able to create such kind of sources (Fig.10 and Fig. 12). Thus, it turned out to be important to apply different meshes to identify unstable solutions.

Furthermore, if a current was impressed into the magnet this mesh dependence was not observed. This becomes clear if we remember that the assumed impressed current of $I_0 = 10\text{ A}$ was calculated by neglecting the resistance of the magnet. On the other hand, this assumption brings us closer to the actual current of $I_{FEM} = 9.43\text{ A}$ calculated by the screw model.

In order to compare the simulation results with the analytical approach, the solutions of the three models were depicted together with the analytical solution from eq. (10) and eq. (13) in Fig. 18 and Fig. 19. It can be seen, that the results for the point model are very close to the analytical approach. This is due to the fact, that in both methods point-like sources are defined. The extension of source and sink to small cylinders leads to lower angular accelerations compared to the point model or the analytical approach. Reason for this is the shortened radial current path between the source and the sink. This yields to less radial current components, which are in combination with the magnetic field causing the torque and hence the angular acceleration.

Another important topic is the definition of the source parameters. The link of the FEM model with a network analysis tool turned out to be an important mod-

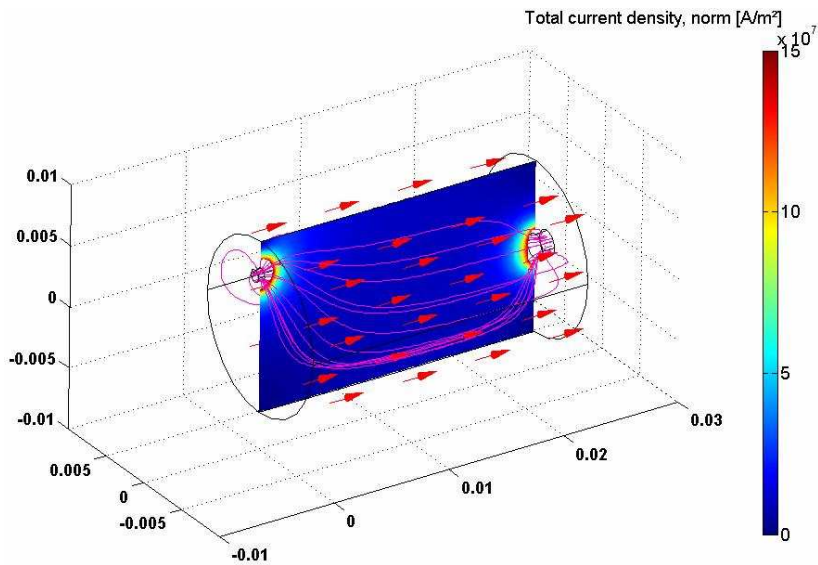


Fig. 20. FEM solution: current flow between extended electrodes, with magnetic flux density (arrows) and total current density (streamlines).

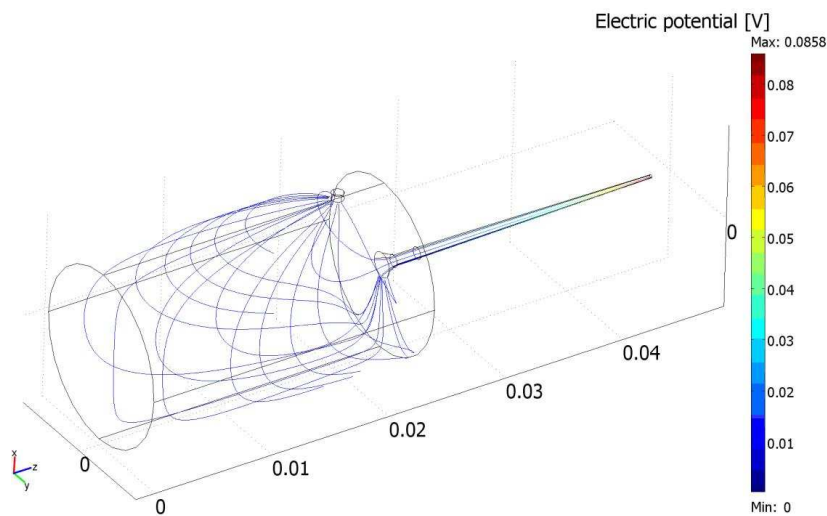


Fig. 21. FEM solution of the SPICE model for the total current density (streamlines), and the distribution of electric potential on the screw (colored scaling).

elling step in order to determine the exact source parameters (see Fig. 20, 21). In order to validate the simulation results an experiment has to be realized to determine the angular acceleration by measuring the angular velocity as a function of time.

8 Conclusion

Both FEM codes can be used to analyse the behaviour of this simple homopolar motor but there are some significant differences. The use of iterative solvers in MAXWELL together with adaptive meshing can cause remarkably higher computational effort and leads to more computing time consumption. Furthermore, parameter variations can be done with MAXWELL very easily, but it is not possible to solve the transient problem related to the rotating magnet. Even if the adaptive meshing is the reason for good results of simulation of point-like electrodes, we have to pay the prize that a relatively high amount of finite elements will be invested in these small regions. Thus, they can no longer be used elsewhere.

The simulations have clearly shown that it could be very important for solving realistic problems, if the FEM code can be combined with circuit analysis tools like SPICE. This can be realized in COMSOL very comfortably. On the other hand, it turned out that it is, in general, very difficult to treat impressed voltages. Thus, first the assumption of impressed currents and applying the SPICE module of COMSOL led to reasonable results, i.e. for the rotating magnet about 70 turns-per-second (after one second) have been estimated finally.

References

- [1] M. Faraday, "New electro-magnetic apparatus," *Quarterly Journal of Science, Literature and the Arts*, vol. XII, pp. 186–187, 1821.
- [2] ———, "Description of an electro-magnetic apparatus for the exhibition of rotatory motion," *Quarterly Journal of Science, Literature and the Arts*, vol. XII, pp. 283–285, 1821.
- [3] L. P. Williams, *The Origin of Field Theory*. Random House, 1966.
- [4] P. A. Davidson, *An Introduction to Magnetohydrodynamics*. Cambridge: Cambridge University Press, 2001.
- [5] *COMSOL Multiphysics - Users Guide, version 3.5*, 2010.
- [6] *MAXWELL v.12 Online Help*, Ansoft, 2009.